Psychotherapy and Psychosomatics

Research Article

Psychother Psychosom
DOI: 10.1159/000552942

Received: October 17, 2025
Accepted: May 31, 2026
Published online: June 8, 2026

How Standardized Is Transcranial Magnetic Stimulation Treatment for Depression? Large-Cohort Modeling Reveals Systematic Dosimetric Variability

Bella Bingbing Zhang[a] Tim Tianze Lin[a] Penny Ping Qin[a] Rebecca Laidi Kan[a] Adam Weili Xia[a] Minxia Jin[a, b] Yinghu Peng[c] Daniel Keeser[d, e, f] on Behalf of CDP Working Group Frank Padberg[d, g] Martin Tik[h, i] Tifei Yuan[j] Benjamin Becker[k, l] Frank Fan Zhu[m] Georg S. Kranz[a, n, o]

[a]Department of Rehabilitation Sciences, The Hong Kong Polytechnic University, Hong Kong, China; [b]Shanghai YangZhi Rehabilitation Hospital (Shanghai Sunshine Rehabilitation Center), School of Medicine, Tongji University, Shanghai, China; [c]Shenzhen Institutes of Advanced Technology, Guangdong-Hong Kong-Macao Joint Laboratory of Human-Machine Intelligence-Synergy Systems, Chinese Academy of Sciences, Shenzhen, China; [d]Department of Psychiatry and Psychotherapy, LMU University Hospital, LMU Munich, Munich, Germany; [e]Max Planck Institute of Psychiatry (MPIP), Munich, Germany; [f]Department of Psychiatry, Psychotherapy, and Psychosomatics, Medical Faculty, University of Augsburg, Augsburg, Germany; [g]DZPG (German Center for Mental Health), Partner Site Munich-Augsburg, Munich/Augsburg, Germany; [h]Center for Medical Physics and BME, Medical University of Vienna, Vienna, Austria; [i]Department of Psychiatry and Behavioral Sciences, Stanford University, Stanford, CA, USA; [j]Shanghai Mental Health Center, Shanghai Jiao Tong University School of Medicine, Shanghai, China; [k]State Key Laboratory of Brain and Cognitive Sciences, The University of Hong Kong, Hong Kong, China; [l]Department of Psychology, The University of Hong Kong, Hong Kong, China; [m]HealthyMind Neuro-Wellness Centre, Hong Kong, China; [n]Mental Health Research Center (MHRC), The Hong Kong Polytechnic University, Hong Kong, China; [o]University Research Facility in Behavioral and Systems Neuroscience (UBSN), The Hong Kong Polytechnic University, Hong Kong, China

Keywords
Transcranial magnetic stimulation · Electric field modeling · Depression · Dosing strategies · Population variability

Abstract

Introduction: Repetitive transcranial magnetic stimulation (rTMS) is a widely utilized, noninvasive brain stimulation technique for treating neurological and psychiatric disorders worldwide. The efficacy of rTMS is influenced by individual head morphology, which shapes the induced electric field (E-field) in the brain. The standard practice for dosing rTMS involves adjusting the intensity to a defined percentage of the motor threshold (MT), a method exemplified by the globally adopted, US FDA-approved protocol of using 120% MT for depression. Since head morphology varies systematically across ethnic groups, current dosing protocols may lead to inconsistent cortical

karger@karger.com
www.karger.com/pps

© 2026 The Author(s).
Published by S. Karger AG, Basel

This article is licensed under the Creative Commons Attribution-NonCommercial 4.0 International License (CC BY-NC) (https://karger.com/Services/OpenAccessLicense). Usage and distribution for commercial purposes requires written permission.

Correspondence to:
Georg S. Kranz, georg.kranz@polyu.edu.hk

Downloaded from http://karger.com/pps/article-pdf/doi/10.1159/000552942/4545790/000552942.pdf by Max Planck Society user on 27 July 2026

dosing. ***Methods:*** Here, we used large-scale computational modeling ($N = 1,085$) to systematically evaluate TMS dosage across "White," "Han Chinese," and "Black or African Am." populations. ***Results:*** Our findings reveal striking ethnic disparities in the E-field ratio between the therapeutic target (left dorsolateral prefrontal cortex, DLPFC) and the calibration site (left primary motor cortex, M1). "Han Chinese" individuals exhibited a significantly higher E-field ratio ($\text{E-field}_{\text{DLPFC}}/\text{E-field}_{\text{M1}} = 1.226$) compared to "White" individuals ($\text{E-field}_{\text{DLPFC}}/\text{E-field}_{\text{M1}} = 1.096$). These differences are primarily driven by variations in scalp-to-cortex distance (SCD). Based on these findings, we derived both simplified population-level adjustment formulas and individualized SCD-based dosing equations and implemented them in a web-based tool for practical use. ***Conclusion:*** Our results suggest that applying a uniform multiplier of MT to DLPFC stimulation may introduce systematic differences in delivered cortical dose across ethnic populations, highlighting that universal dosing conventions derived predominantly from specific demographic cohorts may embed bias, such that established safety and efficacy profiles may not be uniformly applicable across diverse global populations.
© 2026 The Author(s).
Published by S. Karger AG, Basel

Introduction

Repetitive transcranial magnetic stimulation (rTMS) is an effective noninvasive neuromodulation therapy for various neurological and psychiatric disorders including depression [1–6]. It operates on the principle of electromagnetic induction: a magnetic coil placed on the scalp generates a focused electric field (E-field) in the brain, which in turn induces neuronal depolarization. Crucially, the therapeutic efficacy of rTMS is understood to be dose-dependent, depending on the strength of the E-field delivered to the intended cortical target [7]. In the treatment of depression, the primary clinical target is the left dorsolateral prefrontal cortex (DLPFC) [8, 9]. However, the clinical dose for this non-motor target is usually determined indirectly. Standard practice, adopted globally and enshrined in US Food and Drug Administration (FDA)-approved protocols, is to stimulate the DLPFC at an intensity set to 120% of the individual's resting MT (RMT) [3, 10–12]. This RMT is defined as the minimum intensity required to elicit a motor response from the primary motor cortex (M1) [13, 14]. Although the RMT measurement at M1 inherently personalizes the dose to account for anatomical variation at that site, a critical flaw emerges when this is used to infer the dose for the DLPFC. The standard application of a fixed 120% multiplier rests on the implicit premise that the anatomical relationship and tissue properties between these 2 distinct cortical regions are constant across different populations.

Evidence demonstrates that individual head morphology, including the scalp, skull, and cerebrospinal fluid, profoundly shapes the spatial distribution and magnitude of the transcranial magnetic stimulation (TMS) induced E-field [15, 16]. This influence is rooted in fundamental physical principles: the induced E-field attenuates as a function of distance and is further modulated by the heterogeneous conductive properties of the intervening tissue compartments. Consequently, the actual dose reaching the cortex is influenced not only by stimulator output but also by an individual's anatomical geometry [15, 17]. This variability is underscored by computational modeling studies, where fixed-intensity protocols have yielded highly variable cortical E-fields across participants [18].

Importantly, such variability extends beyond individual differences to exhibit population-level patterning. Research in biological anthropology and medical forensics indicates that head and brain morphology vary systematically across ethnic groups [19–22], hinting that the anatomical parameters shaping E-field induction are not uniformly distributed but may instead exhibit subtle divergences across population lineages. Specifically, anthropometric studies of cranial morphology have reported relatively more globular cranial forms in Asian populations compared to more elongated cranial forms in African populations [19]. Given that E-field induction is sensitive to these spatial configurations, such variations may lead to nuanced shifts in the actual dose reaching the cortex across different populations. This, in turn, raises a critical yet overlooked clinical question: if the relative anatomy between M1 and the DLPFC varies systematically with population background, does the current "one-size-fits-all" 120% RMT dosing strategy inadvertently lead to systematic dosing discrepancies? Geriatric rTMS provides a precedent for this possibility. In older cohorts, age-related cortical atrophy [23] tends to increase the scalp-to-cortex distance (SCD), potentially weakening the induced E-field and possibly contributing to the attenuated clinical efficacy observed in these populations [24, 25]. On the other hand, higher stimulation intensity is known to increase the risk of adverse effects, including headaches and seizures [26].

These observations illustrate a broader principle: shared anatomical profiles within a subpopulation can lead to predictable group-level disparities in actual TMS dosing. We therefore hypothesized that systematic

Downloaded from http://karger.com/pps/article-pdf/doi/10.1159/000552942/4545790/000552942.pdf by Max Planck Society user on 27 July 2026

variance in the delivered dose may emerge across ethnic groups, arising as a direct consequence of their distinct anatomical characteristics. To address this question, we conducted a multistage investigation. First, we analyzed an in-house cohort of "White" and "Han Chinese" individuals to quantify differences in TMS-induced E-field delivered to the left DLPFC and to identify key anatomical drivers of its variability. To ensure robustness and generalizability, we validated these findings in an independent cohort of approximately 1,000 individuals, including "White," "Han Chinese," and "Black or African Am." persons, from the Human Connectome Project (HCP-YA) and Chinese Human Connectome Project (CHCP) datasets. We hypothesized that diverse ethnic populations experience different stimulation dosages with FDA-approved rTMS protocols that have been adopted globally.

Methods

Data Sources

High-resolution T1-weighted and T2-weighted structural MRI data were obtained from 2 independent sources. The first dataset comprises our in-house data acquired from "White" and "Han Chinese" participants (shown in online suppl. Table S1, S2; for all online suppl. material, see https://doi.org/10.1159/000552942). This dataset comprised 107 healthy participants: 54 "White" (18 female, 36 male) and 53 "Han Chinese" (33 female, 20 male), aged 22–35 years. The second dataset was derived from public repositories, specifically the Human Connectome Project Yong-Adult (HCP-YA) (https://db.humanconnectome.org) and Chinese Human Connectome Project (CHCP) (https://doi.org/10.11922/sciencedb.01374), which provided high-resolution T1-weighted and T2-weighted images from "White," "Han Chinese" and "Black or African Am." populations, respectively. To ensure age matching between the two datasets, only images of individuals aged 22–35 years were included. Details regarding the scanning parameters for the HCP- and CHCP-derived data are available in the respective original publications.

E-Field Simulation

Structural T1- and T2-weighted images were utilized to generate a three-dimensional volume conductor model for each head using the SimNIBS toolbox (v4.1.0) [17]. The CHARM pipeline was employed for segmentation and volumetric meshing [27]. Each participant's anatomical MRI scans were segmented into nine distinct tissues: scalp, compact bone, spongy bone, cerebrospinal fluid, gray matter, white matter, blood, muscle, and eyeballs (shown in Fig. 1; online suppl. Table S3) [27]. Subsequently, volumetric meshes were generated with the following defined criteria: facet angle = 30°, facet size = 6 mm, facet distance = 0.4 mm, cell radius = 3 mm, and cell size = 8 mm [27]. All segmentation and volumetric meshing outputs were visually inspected and manually checked by experienced researchers with medical background [28]. Subjects exhibiting segmentation artifacts or inaccurate tissue boundary delineations were excluded from the study. Following successful segmentation and meshing, SimNIBS applied the finite-element method to compute the E-field using the assigned tissue conductivity values (shown in Fig. 1; online suppl. Table S3) [27]. We defined the locations of the left DLPFC and the left M1 as the 10-10 EEG positions F3 and C3, respectively [17, 27, 29]. During the simulation, a model of a standard rTMS coil (MagVenture Cool-B65) was positioned over the F3 and C3 scalp locations, oriented at a 45° angle to the sagittal midline with the handle pointing posteriorly [30]. The stimulation intensity was set at 60% maximum stimulator output for DLPFC and 50% maximum stimulator output for M1, consistent with FDA-approved rTMS protocols using a 120% RMT adjustment. Following the simulation, the magnitude of the induced E-field (|E|) was calculated, and the 99th percentile of $|E_{max}|$ was extracted for subsequent data analysis at the cortical projection sites corresponding to F3 ($x = -35.5$, $y = 49.4$, $z = 32.4$ mm) and C3 ($x = -52.2$, $y = -16.4$, $z = 57.8$ mm) in Montreal Neurological Institute (MNI) coordinates [31]. To account for individual variability in cortical excitability, we used the DLPFC/M1 E-field ratio ($E\text{-field}_{DLPFC}/E\text{-field}_{M1}$) as our outcome rather than directly comparing absolute E-field values (shown in Fig. 1). Our rationale for employing this M1-normalized outcome is grounded in long-standing historical tradition [32], expert consensus [33, 34], and established guidelines for TMS dosage determination [35] since stimulation intensity at M1 provides a reliable reference to determine TMS intensity in non-motor targets [34]. The batch scripts used for modeling and analysis are publicly available at https://github.com/nuan750/2026-zhang-TMS-dosimetric-variability.

Exploratory Analysis of Anatomical Factors Related to TMS-Induced E-Field Strength

To investigate anatomical factors associated with interindividual variation in TMS-induced E-field strength, we first quantified the purely geometric SCD, and we then derived a tissue resistance index (RI) that incorporated tissue thickness and conductivity as an

Downloaded from http://karger.com/pps/article-pdf/doi/10.1159/000552942/4545790/000552942.pdf by Max Planck Society user on 27 July 2026

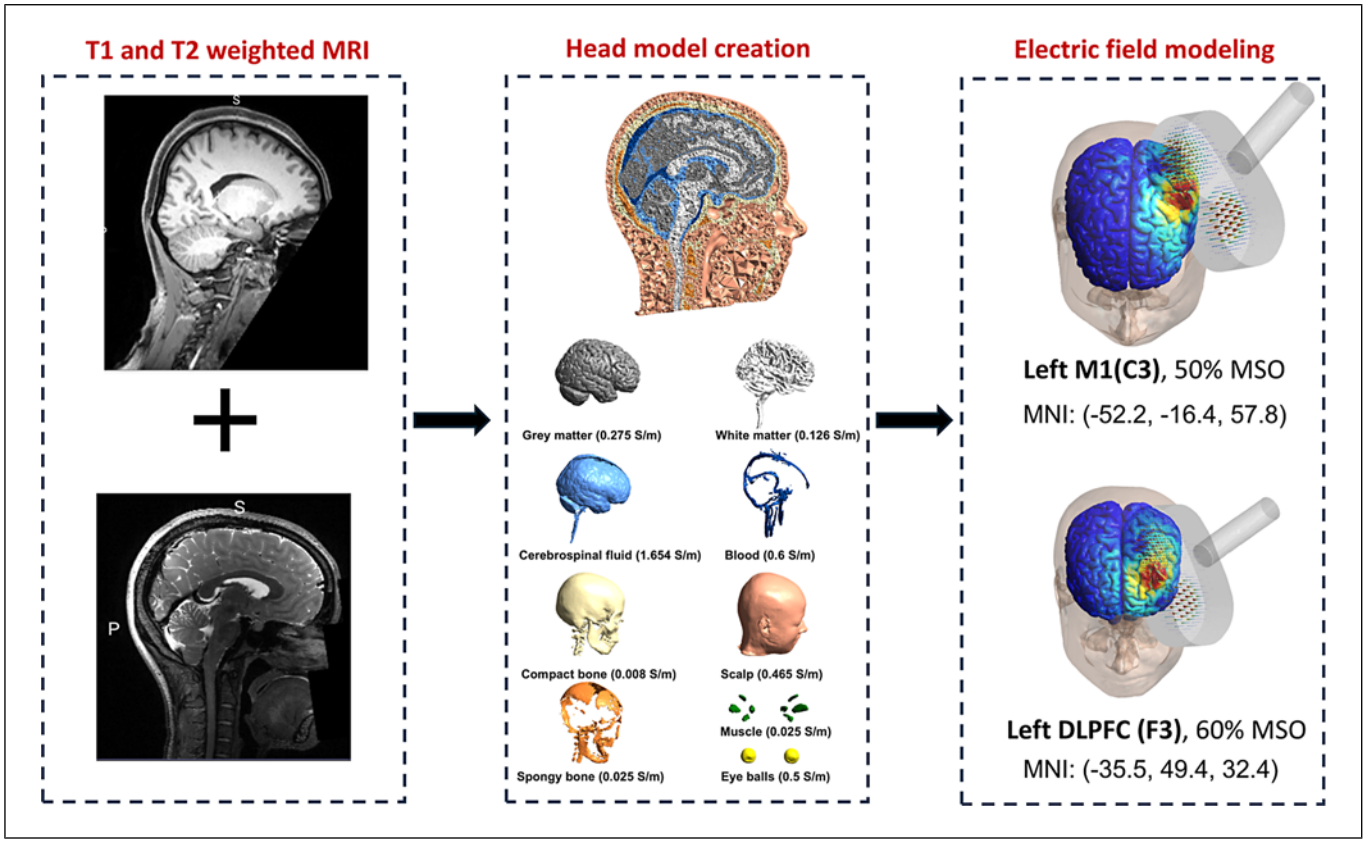


Fig. 1. Pipeline for E-field modeling. Individualized head models are generated from structural MRI images by segmenting multiple tissue types, and are then used to simulate the TMS-induced E-field distribution for targets at the left M1 and left DLPFC.

exploratory surrogate of tissue electrical properties. This sequential approach was used to test whether conductivity-weighted tissue composition could explain variance in E-field strength beyond simple geometric separation.

Tissue Thickness and SCD Extraction

Tissue thickness for each subject was quantified using the GetTissueThickness (GTT) toolbox [36]. This tool enables the extraction of thickness measurements for soft tissue, compact bone, spongy bone, veins, CSF, gray matter, and white matter within a user-defined region of interest (ROI). For our calculation, the ROIs were defined as the positions corresponding to F3 and C3 according to the 10-10 EEG system. Thickness measurements for soft tissue, compact bone, spongy bone, veins, and CSF were extracted for subsequent analysis. The distance was computed as the Euclidean distance between the F3 and C3 scalp positions and the nearest point on the gray matter surface.

Tissue RI

We derived a tissue-specific RI to facilitate comparisons across tissue compartments. Starting from Ohm's law [37, 38], the electrical resistance of a homogeneous slab is estimated by:

$$R = L / (\sigma * A)$$

where L is the thickness of the tissue layer, σ is its electrical conductivity (S m^{-1}), and A is the cross-sectional area perpendicular to current flow. Because all measurements were sampled at an identical MNI target, A can be treated as constant across tissues and therefore cancels out. The RI thus reduces to:

$$RI = L/\sigma$$

which is proportional to a simplified layer-wise resistance and independent of the unknown common area. This derived metric was computed for each tissue layer (soft tissue, bone, veins, CSF). Total RI (RI_{total}) was calculated by summing these individual values.

Downloaded from http://karger.com/pps/article-pdf/doi/10.1159/000552942/4545790/000552942.pdf by Max Planck Society user on 27 July 2026

Statistical Analysis

All statistical analyses were performed using SPSS Statistics 29.0 with a two-tailed alpha level of 0.05 set for all tests. Demographic characteristics were compared across ethnic groups. Pearson's chi-squared (λ^2) test was used to assess the distribution of the categorical variable, gender. For the continuous variable, age, an independent samples *t* test was applied for the two-group comparison in the in-house dataset, while a one-way analysis of variance (ANOVA) was used for the three-group comparison in the large open-access dataset. Our primary hypothesis regarding ethnic differences in E-field strength was tested using an analysis of covariance (ANCOVA). Ethnicity was designated as the fixed factor, while age, gender, and intracranial volume (ICV) were included as covariates to control for their potential confounding effects. If the ANCOVA revealed a significant main effect, post hoc pairwise comparisons with Bonferroni correction were conducted to pinpoint significant differences between specific groups. Crucially, it should be noted that the estimated E-field scales linearly with TMS intensity based on the quasi-static approximation [39, 40]. Consequently, while the absolute stimulation intensity varies across individuals according to their respective MTs, the E-field ratio remains constant for a given subject under the standard 120% RMT adjustment strategy. This physical property ensures that our statistical comparisons of this ratio are robust and independent of the specific dosing intensity used in clinical practice. To explore drivers of E-field variability, multiple linear regressions were constructed predicting E-field strength from SCD and RI_{total}. Beyond these baseline models, we systematically tested: (1) layer-specific RI components, (2) a mean-centered SCD * RI_{total} interaction, and (3) a quadratic term RI_{total}^2 to account for potential localized, interactive, and nonlinear effects. Collinearity was assessed across all models using Variance Inflation Factors.

Results

Standard Treatment Protocol Yields Ethnic Variability in the E-field Ratio

We hypothesized that individuals from different ethnic groups would receive distinct E-field strengths in the left DLPFC (10-10 EEG electrode position F3). To test this, we simulated E-field distributions using 3D head conductor models constructed from individual structural magnetic resonance imaging (MRI) data. Our in-house dataset comprised 107 healthy participants: 54 "White" (18 female, 36 male) and 53 "Han Chinese" (33 female, 20 male), aged 22–35 years. Our in-house dataset was limited to "White" and "Han Chinese" participants, as these were the predominant groups available from our recruitment sites in Hong Kong and from those of our collaborators in their regions. To ensure robustness and generalizability, we replicated our analysis using the HCP and CHCP datasets, which provided 978 T1- and T2-weighted MRI scans: 686 "White" (339 female, 347 male), 141 "Han Chinese" (60 female, 81 male), and 151 "Black or African Am." (89 female, 62 male) participants. Based on prior evidence of head morphology differences, we hypothesized that "Black or African Am." individuals would also exhibit distinct DLPFC/M1 E-field ratios.

In the in-house dataset, E-field strength at DLPFC was 54.991 ± 6.768 V/m and at M1 was 47.569 ± 3.976 V/m in "White' individuals, while in "Han Chinese" individuals, E-field strength at DLPFC was 56.050 ± 5.139 V/m and at M1 was 44.796 ± 4.043 V/m. After controlling for age, gender and ICV, ANCOVA revealed a significant main effect of ethnicity on the DLPFC/M1 E-field ratio ($F_{1,101} = 9.959$, $p = 0.002$, $\eta_p^2 = 0.090$) with "Han Chinese" individuals exhibiting a significantly higher ratio than "White" individuals. Age ($F_{1,101} = 2.722$, $p = 0.102$, $\eta_p^2 = 0.026$), gender ($F_{1,101} = 2.650$, $p = 0.107$, $\eta_p^2 = 0.026$), and ICV ($F_{1,101} = 0.662$, $p = 0.418$, $\eta_p^2 = 0.007$) were not significant covariates (all $p > 0.05$); similarly, the age-by-gender interaction ($F_{1,102} = 0.159$, $p = 0.691$, $\eta_p^2 = 0.002$) was also not significant (shown in Fig. 2).

In the large open-access dataset, E-field strength at DLPFC was 54.123 ± 5.353 V/m and at M1 was 49.596 ± 4.328 V/m in the "White" population, 53.122 ± 5.071 V/m at DLPFC and 43.385 ± 3.866 V/m at M1 in the "Han Chinese" population, and 52.051 ± 5.606 V/m at DLPFC and 45.392 ± 4.751 V/m at M1 in the "Black or African Am." population. The DLPFC/M1 E-field ratio was significantly greater than 1 across all ethnic groups (one-sample *t* tests, all $p < 0.001$), indicating stronger DLPFC stimulation relative to M1 using the current FDA-approved rTMS protocols. We found significant differences in the DLPFC/M1 E-field ratio among ethnic groups ($F_{2,970} = 81.338$, $p < 0.001$, $\eta_p^2 = 0.144$, ANCOVA), with "Han Chinese" exhibiting the highest ratio ($M_{adj} = 1.226$, $SE = 0.010$), followed by "Black or African Am." ($M_{adj} = 1.152$, $SE = 0.009$), while the "White" population exhibits the lowest ratio ($M_{adj} = 1.096$, $SE = 0.004$). Pairwise comparisons confirmed significant differences between all ethnic groups (all $p < 0.001$,

Downloaded from http://karger.com/pps/article-pdf/doi/10.1159/000552942/4545790/000552942.pdf by Max Planck Society user on 27 July 2026

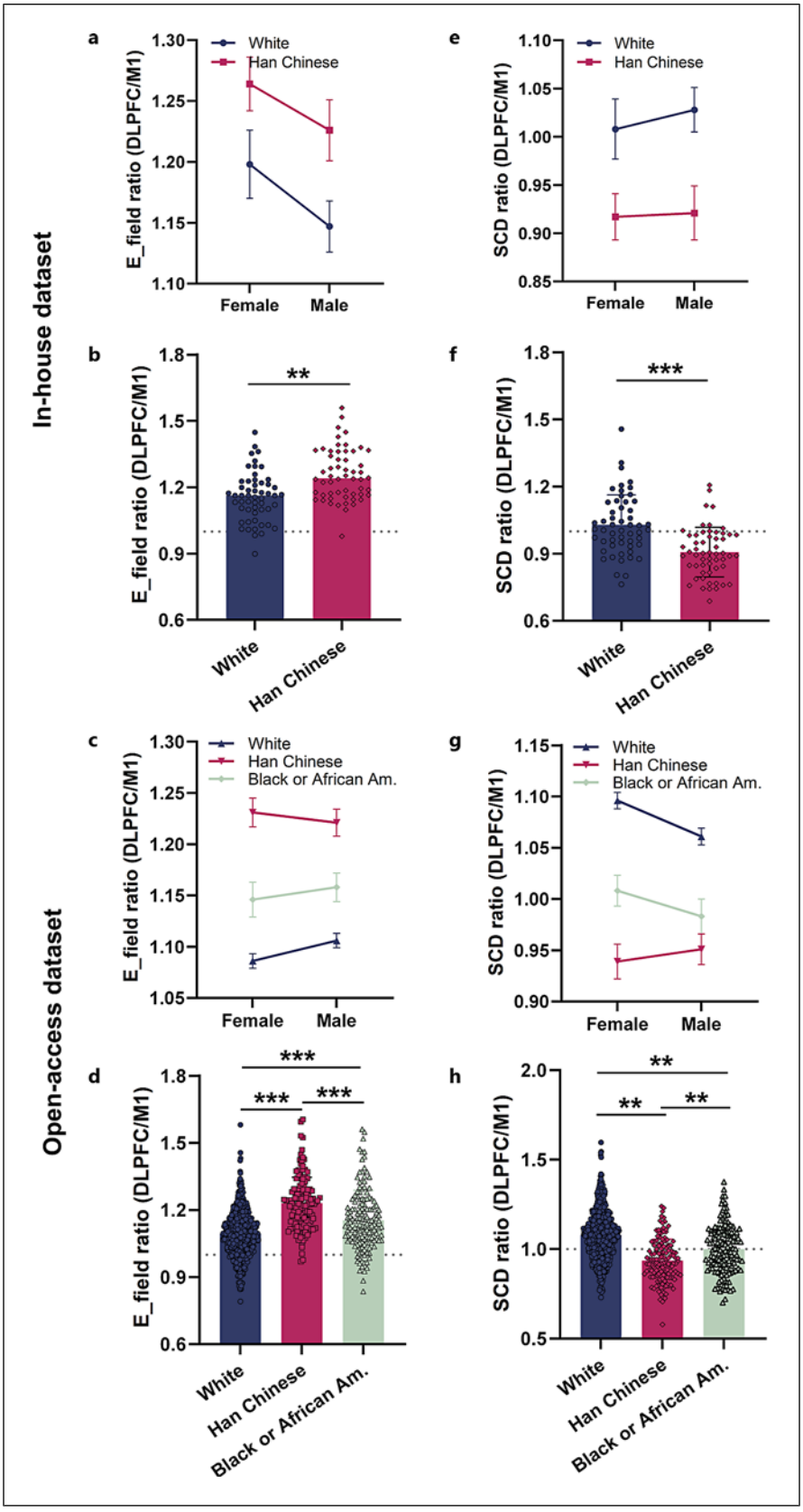


Fig. 2. Comparison of E-field and SCD ratios across different ethnic groups and datasets. The figure compares the E-field ratio (left column, **a–d**) and the scalp-to-cortex distance (SCD) ratio (right column, **e–h**) across different ethnic groups. For both metrics, the upper panels (**a**, **b**, **e**, **f**) display results from our in-house dataset, while the lower panels (**c**, **d**, **g**, **h**) use the open-access datasets. Interaction effects between gender and ethnicity are shown in the line graphs for the in-house (**a**, **e**) and open-access (**c**, **g**) datasets. Main effects of ethnicity are shown in the bar charts for the in-house (**b**, **f**) and open-access (**d**, **h**) datasets. The in-house dataset analyses compare ″White″ and ″Han Chinese″ participants, whereas the open-access dataset analyses compare "White," "Han Chinese," and "Black or African Am." participants. In the line graphs, data points represent the group mean ± standard error of the mean (SEM). In the bar charts, bars indicate the group mean, with individual data points overlaid. $^{**}p < 0.01$, $^{***}p < 0.001$.

Downloaded from http://karger.com/pps/article-pdf/doi/10.1159/000552942/4545790/000552942.pdf by Max Planck Society user on 27 July 2026

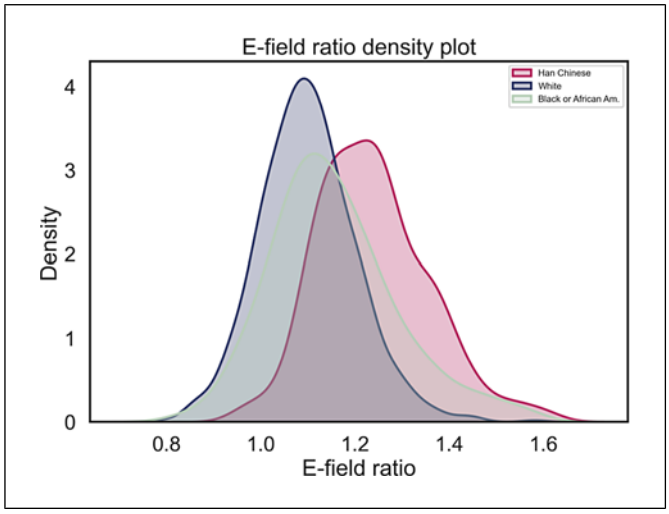


Fig. 3. E-field ratio density plot. Kernel density estimates of the E-field ratio across ethnic groups. Distributions are shown for "Han Chinese" (red), "White" (dark blue), "Black or African Am." (green). The overlap between distributions indicates similarities in E-field ratios.

Bonferroni corrected). Unlike the in-house dataset, age was a significant factor ($F_{1,970}$ = 4.173, p = 0.041, η_p^2 = 0.004) in this large dataset, but gender ($F_{1,970}$ = 0.472, p = 0.492, η_p^2 <0.001), ICV ($F_{1,970}$ = 2.692, p = 0.101, η_p^2 = 0.003) and the ethnicity-by-gender interaction ($F_{2,970}$ = 1.017, p = 0.362, η_p^2 = 0.002) were not significant (shown in Fig. 2).

Descriptive analysis of the E-field ratio distributions revealed a clear separation between the cohorts. The area of overlap between the density plots for "Han Chinese" and "White" participants was approximately 54% (shown in Fig. 3). Probabilistic comparisons further underscored this disparity: there was a 82% probability that a randomly selected "Han Chinese" individual would receive a higher relative stimulation dose than a randomly selected "White" participant. Furthermore, a substantial portion of the ″Han Chinese″ cohort (71.57%) exhibited E-field ratios that exceeded the 75th percentile of the ″White″ cohort, highlighting a systematic upward shift in the dosage received.

To investigate the clinical relevance of these simulated dose variations, we conducted a meta-regression analysis on published studies of left DLPFC rTMS for depression to compare antidepressant efficacy between "White" and "Han Chinese" cohorts (shown in online suppl. Fig. S1, S2; online suppl. Table S4). Ultimately, 51 studies meeting all inclusion criteria were included (shown in online suppl. Fig. S1) [10, 11, 41–89]. Given that most trials did not report ethnicity, cohort ethnicity was primarily inferred from recruitment region and subsequently confirmed by contacting the authors of all included studies to obtain ethnicity data whenever reachable. The meta-regression revealed that ethnicity was a significant predictor of antidepressant effect size (p = 0.004, 95% CI [0.1476, 0.7489]) in the primary model using region-based ethnicity assignments. Specifically, studies with "Han Chinese" participants reported a substantially larger mean effect size (*Hedges'g* = −0.882, 95% CI: [−1.153, −0.611], p < 0.001, I^2 = 78.44%) compared to studies with "White" participants (*Hedges'g* = −0.408, 95% CI [−0.576, −0.240], p < 0.001, I^2 = 62.82%) (shown in online suppl. Fig. S3). Importantly, sensitivity analyses restricted to studies with author-confirmed ethnicity (n = 13) yielded highly consistent results. Ethnicity remained a significant moderator of the treatment effect (p = 0.0014). Specifically, confirmed "Han Chinese" samples continued to exhibit a substantially larger antidepressant effect (Hedges' g = −0.781) compared to "White" samples (Hedges' g = −0.227), demonstrating the robustness and stability of our primary findings (shown in online suppl. Fig. S4). However, given the substantial methodological, institutional, and sociodemographic heterogeneity across studies, these findings provide only indirect, correlational evidence, rather than evidence for direct dose-response relationships. Details of the meta-analysis are provided in the online supplementary materials.

Key Tissue Characteristics Underlying E-Field Variability

A series of multiple linear regression models across both datasets and cortical targets revealed that SCD consistently emerged as the dominant negative predictor of E-field strength (all p < 0.001; shown in Fig. 4; online suppl. Table S5–S8). In the in-house dataset, models incorporating both SCD and RI_{total} explained substantial variance. For the left DLPFC (R^2 = 0.705), SCD remained a highly significant negative predictor (p < 0.001), while the addition of RI provided no significant independent contribution (p = 0.886). A strikingly similar pattern of SCD dominance was observed at the left M1 (R^2 = 0.644), where SCD acted as the sole significant driver of E-field strength, with total RI again showing no independent effect (p = 0.181). These fundamental findings were confirmed in the large open-access dataset. For both the left DLPFC (R^2 = 0.586) and left M1 (R^2 = 0.697), SCD strongly drove the explanatory power as the primary negative predictor (all p < 0.001). While the large sample size rendered the minor effects of RI_{total} and certain layer-specific RIs (e.g., CSF and soft tissue) statistically significant in these models, their additional variance

Downloaded from http://karger.com/pps/article-pdf/doi/10.1159/000552942/4545790/000552942.pdf by Max Planck Society user on 27 July 2026

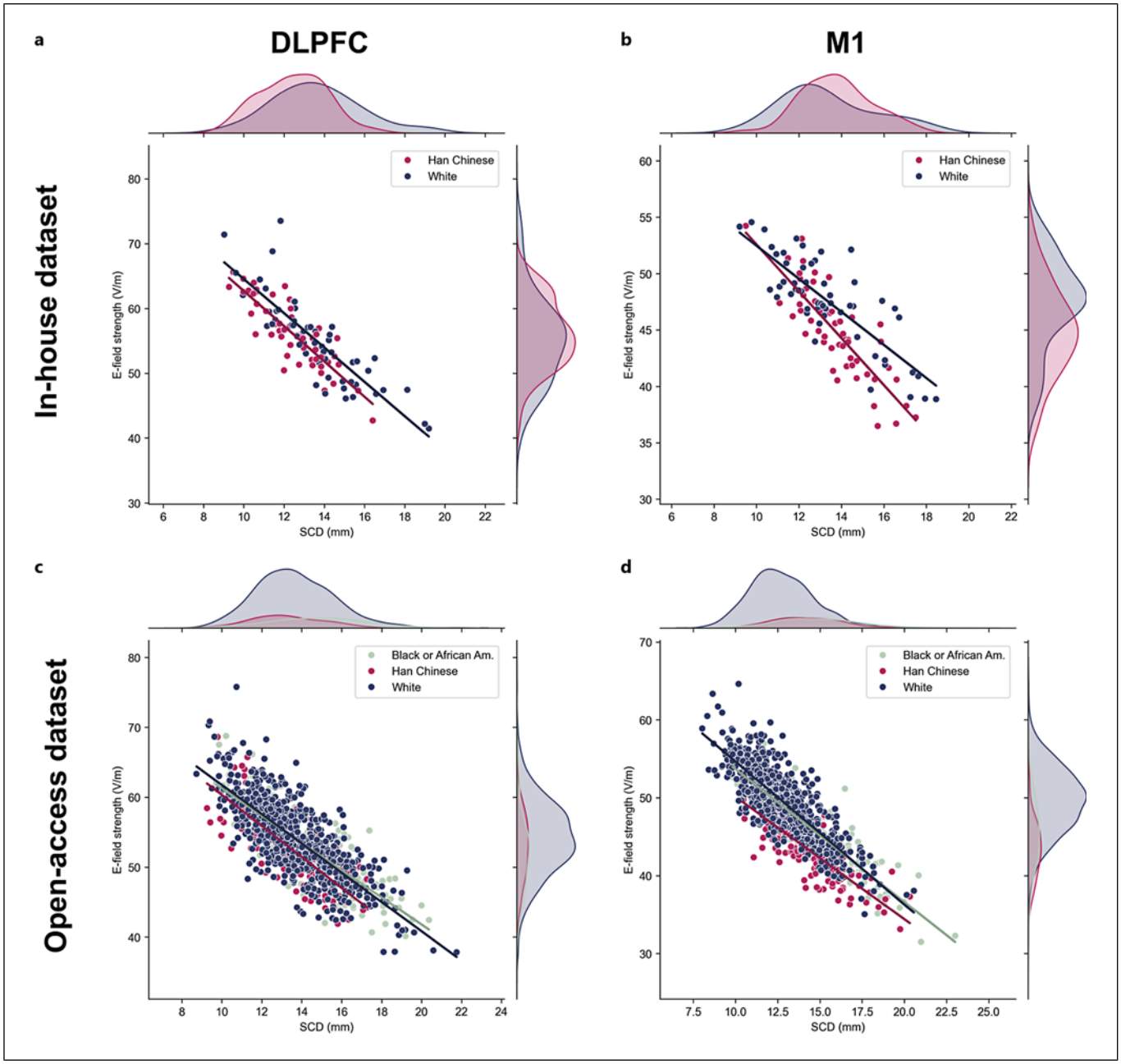


Fig. 4. Scalp-to-cortex distance (SCD) is a primary predictor of TMS-induced E-field strength across different datasets and cortical targets. The figure demonstrates a significant negative correlation between SCD (mm) and induced E-field strength (V/m). The analysis is presented for an in-house dataset (top row, **a**, **b**) and an open-access dataset (bottom row, **c**, **d**), targeting the dorsolateral prefrontal cortex (DLPFC; left column, **a**, **c**) and the primary motor cortex (M1; right column, **b**, **d**). Each joint plot contains a central scatter graph with linear regression lines fitted for different ethnic groups. The in-house dataset (**a**, **b**) includes "Han Chinese" (red) and "White" (dark blue) participants. The open-access dataset (**c**, **d**) includes "Han Chinese" (red), "White" (dark blue), and "Black or African Am." (green) participants. The marginal axes show the kernel density distributions for both SCD and E-field strength for each group.

explained was marginal compared to the robust contribution of SCD. Furthermore, extensive robustness checks incorporating layer-specific RIs, nonlinear terms, and interaction effects confirmed that SCD's primary role is neither an artifact of severe multicollinearity (maximum variance inflation factors <7.2) nor

Downloaded from http://karger.com/pps/article-pdf/doi/10.1159/000552942/4545790/000552942.pdf by Max Planck Society user on 27 July 2026

superseded by specific tissue compositions (detailed in online suppl. Table S5–S8). Taken together, these results establish that SCD is the primary anatomical determinant of E-field strength, irrespective of the cortical target, where a larger SCD predicts a weaker E-field.

Ethnic Variation in SCD of DLPFC Relative to M1

Positing that SCD is the primary determinant of E-field strength, we hypothesized that the observed ethnic differences in the DLPFC/M1 E-field ratio stem from variations in SCD. To test this, we next compared the DLPFC/M1 SCD ratio (SCD_{F3}/SCD_{C3}) across ethnic groups. In the in-house dataset, the raw SCD at left DLPFC and M1 was 13.615 ± 2.184 mm and 13.349 ± 2.211 mm in the "White" population, compared to 12.450 ± 1.616 mm and 13.752 ± 1.626 mm for "Han Chinese" individuals. After controlling for age, gender, and ICV, ANCOVA revealed that "White" population exhibited a significantly larger DLPFC/M1 SCD ratio than the "Han Chinese" population (M_{adj} = 1.018, SE = 0.018 vs. M_{adj} = 0.919, SE = 0.018, $F_{1,101}$ = 15.188, p < 0.001, η_p^2 = 0.131) (shown in Fig. 2). None of the covariates, including age, gender, and ICV, nor the ethnicity-by-gender interaction, reached statistical significance (all p > 0.05). In the large open-access dataset, SCD at left DLPFC was 13.651 ± 1.947 mm and at left M1 was 12.752 ± 1.901 mm in the "White" population, 13.255 ± 1.758 mm at left DLPFC and 14.286 ± 2.025 mm at left M1 in "Han Chinese," and 14.729 ± 2.295 at left DLPFC and 14.861 ± 2.390 mm at left M1 in "Black or African Am." individuals. The ANCOVA confirmed significant differences in the DLPFC/M1 SCD ratio across ethnic groups ($F_{2,970}$ = 67.478, p < 0.001, η_p^2 = 0.122). "White" individuals exhibited the largest SCD ratio (M_{adj} = 1.078, SE = 0.005), indicating greater SCD to the DLPFC than to the M1. In contrast, this relationship was reversed for "Han Chinese" individuals, who showed a ratio below 1 (M_{adj} = 0.945, SE = 0.012). "Black or African Am." individuals had a balanced ratio, with similar distances to both cortices (M_{adj} = 0.995, SE = 0.011). Pairwise comparisons confirmed significant differences between all ethnic groups (all p < 0.01, Bonferroni corrected). In this cohort, age was a significant covariate ($F_{1,970}$ = 6.598, p = 0.010, η_p^2 = 0.007), while gender, ICV, and the ethnicity-by-gender interaction remained nonsignificant (shown in Fig. 2).

Consistency of Results across Different E-Field Metrics

To ensure that our findings were not driven by numerical singularities or mesh discretization artifacts associated with the 99th percentile metric (peak value), we conducted robustness analysis using the 95th percentile and mean E-field values within the target ROI (radius = 10 mm). First, Pearson correlation analysis demonstrated high concordance between the 99th percentile and these alternative metrics across both the in-house and open-access datasets (all p < 0.001; see online suppl. Fig. S5–7). Regarding ethnic differences, analysis in the in-house dataset showed that the E-field ratio followed the same hierarchical pattern as in the primary analysis (Han Chinese > White); however, the difference did not reach statistical significance for either the mean (all p > 0.05) or the 95th percentile (all p > 0.05) (see online suppl. Table S9). This attenuation is plausibly attributable to the inclusion of surrounding, non-focal voxels with lower E-field intensities, which dilutes between-group contrasts and therefore requires larger sample sizes to detect. In contrast, in the larger open-access dataset, statistically significant differences were observed across both metrics (all p < 0.05), fully replicating the hierarchical pattern observed in the primary analysis ("Han Chinese" > "Black or African Am." > "White"; see online suppl. Table S9). Taken together, these results indicate that the observed ethnic hierarchy in modeled E-field strength is robust and reproducible across alternative summary metrics when evaluated in sufficiently powered samples. Furthermore, while variations in mesh resolution and spatial smoothing algorithms can inherently influence peak sensitivity, our methodological pipeline strictly controlled for these computational factors. In all datasets, the average edge length was approximately 0.98 mm (range ~0.7–1.4 mm), which is closely near to the range recommended to keep numerical error below ~2% [90]. In addition, the SimNIBS software intrinsically calculates the E-field using Superconvergent Patch Recovery. This standard finite-element technique improves numerical accuracy through local higher order fitting rather than relying on arbitrary spatial averaging. We therefore expect our findings to remain robust and stable.

Practical Equations for Clinically Precise TMS Dosing at Left DLPFC

Synthesizing the preceding findings, we first established predictive equations to estimate the E-field strength at the left DLPFC and left M1 as a function of stimulator output (dI/dt) for each ethnic group (shown in online suppl. Table S10). Then we calculated simplified, group-level dose-adjustment equations. To achieve E-field equivalence between the 2 sites (E-field_{DLPFC} = E-field_{M1}), the DLPFC stimulation

Downloaded from http://karger.com/pps/article-pdf/doi/10.1159/000552942/4545790/000552942.pdf by Max Planck Society user on 27 July 2026

Table 1. Ethnicity-specific formulas for DLPFC stimulation adjustment

Ethnicity	Population-level adjustment		SCD-based adjustment
	scenario 1: EF strength matched to M1	scenario 2: EF strength matched to White FDA dose	
White	$Stim_adj_{DLPFC} = 108\% \times Stim_{M1}$	$Stim_adj_{DLPFC} = 120\% \times Stim_{M1}$	$Stim_adj_{DLPFC} = Stim_{M1} \times (1.063 + 0.030 \times \Delta d)$
Han Chinese	$Stim_adj_{DLPFC} = 96\% \times Stim_{M1}$	$Stim_adj_{DLPFC} = 108\% \times Stim_{M1}$	$Stim_adj_{DLPFC} = Stim_{M1} \times (1.001 + 0.030 \times \Delta d)$
Black or African Am	$Stim_adj_{DLPFC} = 104\% \times Stim_{M1}$	$Stim_adj_{DLPFC} = 115\% \times Stim_{M1}$	$Stim_adj_{DLPFC} = Stim_{M1} \times (1.047 + 0.039 \times \Delta d)$

This table summarizes ethnicity-specific formulas for adjusting DLPFC stimulation intensity relative to M1 using two complementary approaches. In the population-level approach, fixed scaling factors were derived from group-level electric field (EF) relationships. In the SCD-based approach, the adjusted DLPFC intensity is individualized according to the inter-target SCD difference (Δd). In Scenario 1, the goal was to set the DLPFC stimulation intensity such that the induced E-field at the DLPFC matched the induced EF at M1 within the same ethnicity. In Scenario 2, the goal was to match the DLPFC EF exposure associated with the FDA-approved stimulation intensity of 120% resting motor threshold (RMT) in the ″White″ population. Specifically, the DLPFC E-field produced by 120% RMT in ″White″ participants was used as the reference exposure, and the corresponding stimulation intensities required to achieve the same DLPFC EF were then estimated for the ″Han Chinese″ and ″Black or African Am.″ populations. In all formulas, $Stim_adj_{DLPFC}$ denotes the adjusted stimulation intensity for the DLPFC, $Stim_{M1}$ denotes the di/dt value corresponding to the individual motor-threshold stimulation intensity over M1, and Δd represents the individual DLPFC-minus-M1 SCD difference. These formulas were derived from simulations performed with the MagVenture MagPro ×100 stimulator and Cool-B65 coil and may not be directly generalizable to other stimulator-coil configurations. The FDA-approved 120% RMT reference was motivated by prior randomized controlled trials in predominantly ″White″ samples.

intensity relative to an individual's MT-based output would require multiplication by 1.080 for "White" individuals, 0.963 for "Han Chinese," and 1.035 for "Black or African Am." individuals. Alternatively, to match the specific DLPFC/M1 E-field ratio observed in the "White" cohort under the standard FDA-approved 120% RMT dosing strategy, the required adjustment factors were 1.08 for "Han Chinese" individuals and 1.15 for "Black or African Am." individuals (shown in Table 1). Furthermore, to echo the classic distance-adjustment framework proposed by Stokes and colleagues [91], we additionally developed SCD-informed individualized equations. When SCD information is available, the required DLPFC output can be estimated using ethnic-specific linear models expressed as $Stim_adj_{DLPFC} = Stim_{M1} \times (A + B \times \Delta d)$, where Δd represents the individual DLPFC-minus-M1 SCD difference (shown in Table 1, online suppl. Section 4, and online suppl. Table S11). To facilitate the practical application of both approaches, we developed a user-friendly web-based tool (shown in Fig. 5, https://calculator-dosage.vercel.app/). Users can automatically obtain the recommended DLPFC stimulation intensity derived from our models by inputting a subject's ethnicity, with the option to include SCD data for a more individualized adjustment.

Discussion

Our findings demonstrate that applying a universal fixed multiplier (e.g., 120%) to the MT introduces significant disparities in the delivered E-field dose at the DLPFC across different ethnic groups. Specifically, "Han Chinese" individuals exhibited the highest DLPFC/M1 E-field ratio (1.226) whereas "White" individuals had the lowest ratio (1.096). These differences are primarily driven by variations in SCD: "White" individuals demonstrated a greater relative SCD over the DLPFC compared to M1, while "Han Chinese" individuals exhibited a smaller relative SCD. Critically, the differences in rTMS dose were mirrored in the antidepressant responses to rTMS therapy.

Our observed population-level variability in TMS dosing may provide critical insights into refining future safety guidelines. When simulating a standardized 120% RMT dose at the DLPFC, the ″Han Chinese″ cohort received a relative E-field exposure mathematically equivalent to a 134% RMT dose in the ″White″ population. Current international guidelines recommend an intensity of 80%–120% RMT as safe for theta-burst stimulation [34]. Because the nominal 120% RMT

Downloaded from http://karger.com/pps/article-pdf/doi/10.1159/000552942/4545790/000552942.pdf by Max Planck Society user on 27 July 2026



Fig. 5. Interface of the bilingual web-based TMS precision dosing tool for DLPFC. **a** Top section of the interface with the tool title and brief introduction. **b** Patient profile and reference input module, in which users enter ethnicity and M1 stimulation intensity. **c** Methodology and parameter-setting module for the individualized SCD-based model. **d** Methodology and parameter-setting module for the population-level model. **e** Output panel displaying the recommended DLPFC stimulation intensity and the corresponding estimation formula.

dose is routinely and safely administered in ″Han Chinese″ clinical cohorts, our findings provide indirect but compelling evidence that a biophysical exposure equivalent to roughly 134% RMT (relative to the ″White″ population standard) may, in fact, remain within safe physiological limits. Beyond this specific example, our findings highlight a profound systemic issue. Universal guidelines derived predominantly from specific demographic cohorts likely harbor inherent anatomical biases. Consequently, established safety and efficacy profiles may not seamlessly translate across diverse global populations. Accounting for these morphological differences is therefore warrants consideration to improve the validity of quantitative comparisons in future research.

While individualized E-field modeling represents the optimal future of precise TMS dosing, its reliance on advanced neuroimaging and computational expertise makes it largely inaccessible for most clinical settings. To address dose variability without such resources, additive distance-adjusted formulas (e.g., Stokes et al. [91]) are frequently used. However, by relying on a fixed additive constant, this approach overlooks the nonlinear decay of electromagnetic fields. Consequently, it leads to severe E-field variability both within individuals across targets and between individuals for the same target [92]. In

Downloaded from http://karger.com/pps/article-pdf/doi/10.1159/000552942/4545790/000552942.pdf by Max Planck Society user on 27 July 2026

contrast, our SCD-based formula better accounts for this physical variability by equating the actual E-field dose reaching the target cortex. Furthermore, because our adjustment is anchored to the individual's MT, a critical functional marker of cortical excitability, our strategy integrates both structural and functional perspectives. In addition, our method follows the multiplicative nature of electromagnetic decay. Yet, recognizing that utilizing this formula still requires individual MRI to measure cortical depth, we also derived MRI-free, group-level dose-adjustment methods. Ultimately, this dual-tiered framework serves as a highly practical heuristic, bridging the critical gap between advanced biophysical modeling and widespread clinical practice. However, given these benchmarks were derived using the MagVenture Cool-B65 coil (handle pointing posterior-left), caution is warranted when extrapolating to other coil geometries or orientations.

Our analyses establish that SCD overwhelmingly dominates the RI in explaining E-field variability. This aligns perfectly with TMS biophysics: primary magnetic fields pass unimpeded through biological tissues, meaning physical spatial decay, captured directly by SCD, largely contribute to field attenuation before reaching the cortex [24, 91]. While massive samples revealed minor RI effects (e.g., from CSF), their overall contribution remains marginal. Ultimately, intracranial E-fields are predominantly shaped by complex 3D compartment boundaries (particularly skull-CSF and CSF-GM interfaces) more so than the simple 1D aggregate of tissue resistance estimated by RI [93–95].

While some literature has highlighted broad gender differences in TMS dosing metrics by reporting shorter SCD and stronger E-fields in females [96], a closer examination of their underlying data reveals a highly specific alignment with our results. In their comprehensive analysis, when measurements were normalized to the M1 to create relative metrics (equivalent to our F3/C3 ratio), significant gender differences were notably absent at the F3 target. Our primary findings corroborate this localized lack of gender effect. By evaluating the relative E-field and SCD ratios (F3/C3) across a multi-ethnic cohort, our rigorous ANCOVA models found no significant main effect of gender. Importantly, to explicitly investigate the potential confounding role of head size, we compared models with and without ICV as a covariate. Notably, in our exploratory models omitting ICV, a superficial gender effect emerged in the in-house dataset (see online suppl. Table S12). However, accounting for ICV as a covariate rendered this effect nonsignificant, harmonizing the findings across both the in-house and open datasets. This comparison suggests that the apparent gender differences observed in these specific TMS metrics may be largely attributable to underlying disparities in gross anatomical volume, rather than stemming solely from biological sex. Consequently, these results underscore the importance of incorporating anatomical covariates to better distinguish potential physiological effects from baseline structural variances.

While our findings highlight systematic ethnicity-related influences on TMS dosing, these deviations must be contextualized within the broader landscape of clinical variability [92]. In routine practice, dosing fluctuations frequently arise from methodological factors, such as positioning errors and operator variability, alongside natural intraindividual shifts in cortical excitability over time [97]. Consequently, while E-field modeling effectively improves dosing precision, a purely structural approach cannot fully capture this dynamic complexity. The ultimate effects of TMS are functional outcomes, which are simultaneously modulated by ongoing brain states, functional network activity, and other factors, introducing significant variance even when the E-field magnitude is held constant. Furthermore, differences in local boundary conditions, such as the cerebrospinal fluid-gray matter interface, and variations in pyramidal nerve fiber orientation may alter physiological efficacy across different cortical targets. Therefore, a normalized E-field ratio does not strictly equate to an equivalent TMS effect. Ultimately, achieving consistent clinical outcomes across diverse populations requires moving beyond solely E-field-informed dosing by integrating functionally informed approaches, such as concurrent neuroimaging or EEG, in both experimental and clinical settings [98, 99].

Several limitations of the present study warrant consideration. First, our investigation was confined to the left DLPFC. This focus was chosen to enhance the immediate clinical relevance of our findings, given its status as the primary FDA-approved target for depression. Nonetheless, as the therapeutic applications of rTMS continue to expand, it would be valuable for future research to extend this modeling approach to other emerging non-motor targets, such as the right DLPFC or the medial prefrontal cortex. Second, we defined DLPFC and M1 targets using standard scalp-based F3 and C3 locations rather than individualized functional targets. Although this approach maximizes clinical practicality and reflects the most common non-neuronavigated TMS practice, scalp-based coordinates may map differently to the underlying cortex across populations. Consequently, differences in cranial morphology could introduce

Downloaded from http://karger.com/pps/article-pdf/doi/10.1159/000552942/4545790/000552942.pdf by Max Planck Society user on 27 July 2026

localization errors that propagate into the simulated E-fields and derived dosing equations, underscoring the need for future validation using individualized neuronavigated targets. Third, while our work suggests that dose variations may be associated with broad factors such as ethnicity, it is important to note that interindividual variability also exists within any given population. Consequently, achieving true personalization appears to be a logical long-term objective for the field. Our findings therefore lend support to the rationale for MRI-guided rTMS, wherein an individual's structural scan could be used to inform treatment planning and personalize the dose. A significant barrier remains, however: the precise, therapeutically optimal E-field magnitude required at the cortex is still largely unknown. As such, establishing this "target dose" through carefully designed clinical trials that correlate E-field strength with clinical outcomes appears to be a critical next step for refining the clinical application of rTMS. Fourth, in calculating the tissue RI, we made the simplifying assumption that the cross-sectional area (A) at the MNI target coordinate is constant across individuals. In reality, electric current is distributed throughout a three-dimensional volume, meaning that individual variations in head and tissue geometry can alter both the effective cross-sectional area and the current's path. Consequently, the true tissue resistance may exhibit variations that our single-point RI metric cannot fully account for. However, this approximation was necessitated by our methodology, which involved extracting E-field values at a single coordinate for all subjects. Finally, we emphasize that ethnicity should be regarded only as a coarse proxy for population-level variation in anatomically relevant features, rather than as a biological essence or a stand-alone basis for treatment assignment. These findings must not be misused to support pseudoscientific claims or any form of racial categorization. Our results suggest that a uniform "one-size-fits-all" dosing strategy leads to systematic discrepancies in the dose delivered to the cortex across populations. Recognizing these group-level tendencies is therefore crucial, as it provides a necessary foundation for tailored dosing adjustments that ensure clinical safety and efficacy across diverse patient backgrounds.

Conclusion

Our study shows that the conventional "one-size-fits-all" dosing strategy for rTMS therapy systematically produces variable E-field delivery at the left DLPFC leading to inconsistent treatment dosage. Our findings highlight SCD as a primary contributor to this observed variability. These results underscore the need to explore personalized, anatomy-informed dosing strategies, which may hold the potential to improve treatment outcomes and reduce response heterogeneity. The methods and models presented here offer a potential pathway toward this goal, with the aim of ultimately fostering a more reliable and effective application of rTMS for patients with neuropsychiatric disorders.

Acknowledgments

The authors would like to thank Manxinyu Shi for her assistance with this study. We would also like to thank the following members of the CDP working group for their support (listed in alphabetical order by last name): Emanuel Boudriot, Joanna Moussiopoulou, Florian Raabe, Lukas Roell, Elias Wagner, and Vladislav Yakimov.

Statement of Ethics

This was a simulation study based on pre-existing and fully anonymized MRI structural data. As this research involved the analysis of secondary, de-identified data and did not involve any new human subjects, it was exempt from requiring new institutional review board (IRB) approval according to institutional guidelines. All data utilized in this study were sourced from previous studies that were conducted in accordance with the Declaration of Helsinki. The original data collection protocols were approved by their respective IRBs, and written informed consent was obtained from all participants at the time of their original enrollment. Specifically, the original collection of the in-house Han Chinese population dataset was approved by the Institutional Review Board of The Hong Kong Polytechnic University (Approval Nos: HSEARS20220808002, HSEARS20220816001-03, HSEARS20240319006, HSEARS20231218001). The original collection of the White cohort dataset was approved by the Ethics Committees of LMU University Hospital, LMU Munich, Germany (project numbers 20-0528 and 22-0035), and the Local Ethics Committee of the Medical University of Vienna, Austria (Approval Nos: 1309/2018).

Conflict of Interest Statement

F.P. is a member of the European Scientific Advisory Board of Brainsway Inc., Jerusalem, Israel, and the International Scientific Advisory Board of Sooma, Helsinki, Finland. He has received speaker's honoraria from Mag and More GmbH, the neuroCare Group, Munich, Germany, and Brainsway Inc. His laboratory has received support with equipment from neuroConn GmbH, Ilmenau, Germany, Mag and More GmbH, and Brainsway Inc. G.K. received honoraria from Storz medical, the Academy of brain stimulation, Healthlink holdings. B.B.B.Z. and R.L.D.K. received honoraria from the Academy of brain stimulation. B.B.B.Z. received Eurasia-Pacific Ernst Mach Scholarship from

Downloaded from http://karger.com/pps/article-pdf/doi/10.1159/000552942/4545790/000552942.pdf by Max Planck Society user on 27 July 2026

Austria's Agency for Education and Internationalisation. P.P.Q. received honoraria from Storz medical. All other authors reported no potential conflicts of interest. BB was a member of the journal's Editorial Board at the time of submission.

Funding Sources

This work was supported by the General Research Fund (No. 15106222) and the Strategic Topics Grant (TG1/M-501/ 23-N) under the University Grands Committee of the HKSAR, the Mental Health Research Center (No. 0048822 and 0040786), the University Research Facility in Behavioral and Systems Neuroscience (Inbound Capacity Building Scheme), and the Department of Rehabilitation Sciences (No. 0055985 and 0042417) of The Hong Kong Polytechnic University. The funders had no role in the design, data collection, data analysis, and reporting of this study.

Author Contributions

B.B.B.Z.: conceptualization, data curation, investigation, formal analysis, software, visualization, methodology, writing – original draft, and writing – review and editing; T.T.Z.L.: conceptualization, data curation, investigation, software, methodology, formal analysis, validation, writing – original draft, and writing – review and editing. P.P.Q.: investigation, software, validation, writing – review and editing; R.L.D.K.: investigation, formal analysis, software, visualization, methodology, and writing – review and editing; J.M.X.: investigation, validation, and writing – review and editing; Y.H.P.: software, validation, visualization, and writing – review and editing; A.W.L.X.: investigation, validation, and writing – review and editing; D.K. and M.T.: data curation, resources, validation, writing – original draft, and writing – review and editing; F.P.: conceptualization, resources, methodology, writing – original draft, and writing – review and editing; T.Y., B.B., and F.F.Z.: conceptualization, methodology, writing original draft, and writing – review and editing; G.S.K.: conceptualization, writing – original draft, writing – review and editing, resources, supervision, and project administration.

Data Availability Statement

The data that support the findings of this study include in-house proprietary datasets and publicly available datasets. The three in-house datasets are not publicly available due to participant privacy and the data sharing policies of the originating institutions. However, access to these datasets can be requested through the corresponding author. Any data sharing is subject to a formal data use agreement and requires the approval of the respective principal investigators who collected the data (G.S.K. for the in-house Chinese dataset; M.T. and D.K. for the in-house White dataset). The public datasets analyzed in this study were sourced from the Human Connectome Project (HCP) and the Chinese Human Connectome Project (CHCP). The head models generated from all datasets (both in-house and public) are available from the corresponding author upon reasonable request. Data acquired at the Medical University of Vienna, Austria, will be made available via author M.T. upon reasonable request and in accordance with the local IRB. The interactive tool is available at https://calculator-dosage.vercel.app/.

References

1 Hallett M. Transcranial magnetic stimulation and the human brain. Nature. 2000;406(6792):147–50. https://doi.org/10.1038/35018000
2 Machado S, Arias-Carrión O, Paes F, Vieira RT, Caixeta L, Novaes F, et al. Repetitive transcranial magnetic stimulation for clinical applications in neurological and psychiatric disorders: an overview. Eurasian J Med. 2019;45(3):191–206. https://doi.org/10.5152/eajm.2013.39
3 Lefaucheur J-P, Aleman A, Baeken C, Benninger DH, Brunelin J, Di Lazzaro V, et al. Evidence-based guidelines on the therapeutic use of repetitive transcranial magnetic stimulation (rTMS): an update (2014–2018). Clin Neurophysiol. 2020;131(2):474–528. https://doi.org/10.1016/j.clinph.2019.11.002
4 Kishi T, Ikuta T, Sakuma K, Hatano M, Matsuda Y, Wilkening J, et al. Theta burst stimulation for depression: a systematic review and network and pairwise meta-analysis. Mol Psychiatry. 2024;29(12):3893–9. https://doi.org/10.1038/s41380-024-02630-5
5 Cole E, O'Sullivan SJ, Tik M, Williams NR. Accelerated Theta burst stimulation: safety, efficacy, and future advancements. Biol Psychiatry. 2024;95(6):523–35. https://doi.org/10.1016/j.biopsych.2023.12.004
6 Chen L, Klooster DCW, Tik M, Thomas EHX, Downar J, Fitzgerald PB, et al. Accelerated repetitive transcranial magnetic stimulation to treat major depression: the past, present, and future. Harv Rev Psychiatry. 2023;31(3):142–61. https://doi.org/10.1097/hrp.0000000000000364
7 Fatemi-Ardekani A. Transcranial magnetic stimulation: physics, electrophysiology, and applications. Crit Rev Biomed Eng. 2008;36(5–6):375–412. https://doi.org/10.1615/critrevbiomedeng.v36.i5-6.30
8 Brunoni AR, Chaimani A, Moffa AH, Razza LB, Gattaz WF, Daskalakis ZJ, et al. Repetitive transcranial magnetic stimulation for the acute treatment of major depressive episodes: a systematic review with network meta-analysis. JAMA Psychiatry. 2017;74(2):143–52. https://doi.org/10.1001/jamapsychiatry.2016.3644
9 Kan RLD, Padberg F, Giron CG, Lin TTZ, Zhang BBB, Brunoni AR, et al. Effects of repetitive transcranial magnetic stimulation of the left dorsolateral prefrontal cortex on symptom domains in neuropsychiatric disorders: a systematic review and cross-diagnostic meta-analysis. Lancet Psychiatry. 2023;10(4):252–9. https://doi.org/10.1016/s2215-0366(23)00026-3
10 George MS, Lisanby SH, Avery D, McDonald WM, Durkalski V, Pavlicova M, et al. Daily left prefrontal transcranial magnetic stimulation therapy for major depressive disorder: a Sham-controlled randomized trial. Arch Gen Psychiatry. 2010;67(5):507–16. https://doi.org/10.1001/archgenpsychiatry.2010.46
11 O'Reardon JP, Solvason HB, Janicak PG, Sampson S, Isenberg KE, Nahas Z, et al. Efficacy and safety of transcranial magnetic stimulation in the acute treatment of major depression: a multisite randomized controlled trial. Biol Psychiatry. 2007;62(11):1208–16. https://doi.org/10.1016/j.biopsych.2007.01.018
12 Blumberger DM, Vila-Rodriguez F, Thorpe KE, Feffer K, Noda Y, Giacobbe P, et al. Effectiveness of theta burst versus high-frequency repetitive transcranial magnetic stimulation in patients with depression (THREE-D): a randomised non-inferiority trial. Lancet. 2018;391(10131):1683–92. https://doi.org/10.1016/s0140-6736(18)30295-2

Downloaded from http://karger.com/pps/article-pdf/doi/10.1159/000552942/4545790/000552942.pdf by Max Planck Society user on 27 July 2026

13 Rothwell JC, Hallett M, Berardelli A, Eisen A, Rossini P, Paulus W. Magnetic stimulation: motor evoked potentials. The International federation of clinical neurophysiology. Electroencephalogr Clin Neurophysiol Suppl. 1999;52:97–103.
14 Rossini PM, Barker A, Berardelli A, Caramia M, Caruso G, Cracco R, et al. Non-invasive electrical and magnetic stimulation of the brain, spinal cord and roots: basic principles and procedures for routine clinical application. Report of an IFCN committee. Electroencephalogr Clin Neurophysiol. 1994; 91(2):79–92. https://doi.org/10.1016/0013-4694(94)90029-9
15 Thielscher A, Opitz A, Windhoff M. Impact of the gyral geometry on the electric field induced by transcranial magnetic stimulation. Neuroimage. 2011;54(1):234–43. https://doi.org/10.1016/j.neuroimage.2010.07.061
16 Miranda PC, Hallett M, Basser PJ. The electric field induced in the brain by magnetic stimulation: a 3-D finite-element analysis of the effect of tissue heterogeneity and anisotropy. IEEE Trans Biomed Eng. 2003;50(9):1074–85. https://doi.org/10.1109/tbme.2003.816079
17 Thielscher A, Antunes A, Saturnino GB. Field modeling for transcranial magnetic stimulation: a useful tool to understand the physiological effects of TMS? Annu Int Conf IEEE Eng Med Biol Soc. 2015;2015:222–5.
18 Evans C, Bachmann C, Lee JS, Gregoriou E, Ward N, Bestmann S. Dose-controlled tDCS reduces electric field intensity variability at a cortical target site. Brain Stimul. 2020;13(1): 125–36. https://doi.org/10.1016/j.brs.2019.10.004
19 Matsumura H, Tanijiri T, Kouchi M, Hanihara T, Friess M, Moiseyev V, et al. Global patterns of the cranial form of modern human populations described by analysis of a 3D surface homologous model. Sci Rep. 2022;12(1):13826. https://doi.org/10.1038/s41598-022-15883-3
20 Ball R, Shu C, Xi P, Rioux M, Luximon Y, Molenbroek J. A comparison between Chinese and Caucasian head shapes. Appl Ergon. 2010;41(6):832–9. https://doi.org/10.1016/j.apergo.2010.02.002
21 Cao G, Zhang S, He Z, Wang Z, Guo L, Yan Z, et al. Gyral peak variations between HCP and CHCP: functional and structural implications. Brain Struct Funct. 2025;230(2): 37. https://doi.org/10.1007/s00429-025-02894-9
22 Jong L. On the persistence of race: unique skulls and average tissue depths in the practice of forensic craniofacial depiction. Soc Stud Sci. 2023;53(6):891–915. https://doi.org/10.1177/03063127221112073
23 Gur RC, Mozley PD, Resnick SM, Gottlieb GL, Kohn M, Zimmerman R, et al. Gender differences in age effect on brain atrophy measured by magnetic resonance imaging. Proc Natl Acad Sci USA. 1991;88(7):2845–9. https://doi.org/10.1073/pnas.88.7.2845
24 Kozel FA, Nahas Z, deBrux C, Molloy M, Lorberbaum JP, Bohning D, et al. How coil-cortex distance relates to age, motor threshold, and antidepressant response to repetitive transcranial magnetic stimulation. J Neuropsychiatry Clin Neurosci. 2000;12(3): 376–84. https://doi.org/10.1176/jnp.12.3.376
25 Figiel GS, Epstein C, McDonald WM, Amazon-Leece J, Figiel L, Saldivia A, et al. The use of rapid-rate transcranial magnetic stimulation (rTMS) in refractory depressed patients. J Neuropsychiatry Clin Neurosci. 1998;10(1):20–5. https://doi.org/10.1176/jnp.10.1.20
26 Machii K, Cohen D, Ramos-Estebanez C, Pascual-Leone A. Safety of rTMS to non-motor cortical areas in healthy participants and patients. Clin Neurophysiol. 2006; 117(2):455–71. https://doi.org/10.1016/j.clinph.2005.10.014
27 Puonti O, Van Leemput K, Saturnino GB, Siebner HR, Madsen KH, Thielscher A. Accurate and robust whole-head segmentation from magnetic resonance images for individualized head modeling. Neuroimage. 2020;219:117044. https://doi.org/10.1016/j.neuroimage.2020.117044
28 Caulfield KA, Li X, George MS. A re-examination of motor and prefrontal TMS in tobacco use disorder: time for personalized dosing based on electric field modeling? Clin Neurophysiol. 2021;132(9):2199–207. https://doi.org/10.1016/j.clinph.2021.06.015
29 Jurcak V, Tsuzuki D, Dan I. 10/20, 10/10, and 10/5 systems revisited: their validity as relative head-surface-based positioning systems. Neuroimage. 2007;34(4):1600–11. https://doi.org/10.1016/j.neuroimage.2006.09.024
30 Drakaki M, Mathiesen C, Siebner HR, Madsen K, Thielscher A. Database of 25 validated coil models for electric field simulations for TMS. Brain Stimul. 2022;15(3): 697–706. https://doi.org/10.1016/j.brs.2022.04.017
31 Okamoto M, Dan H, Sakamoto K, Takeo K, Shimizu K, Kohno S, et al. Three-dimensional probabilistic anatomical cranio-cerebral correlation via the international 10-20 system oriented for transcranial functional brain mapping. Neuroimage. 2004;21(1):99–111. https://doi.org/10.1016/j.neuroimage.2003.08.026
32 Turi Z, Lenz M, Paulus W, Mittner M, Vlachos A. Selecting stimulation intensity in repetitive transcranial magnetic stimulation studies: a systematic review between 1991 and 2020. Eur J Neurosci. 2021;53(10): 3404–15. https://doi.org/10.1111/ejn.15195
33 Wassermann EM. Risk and safety of repetitive transcranial magnetic stimulation: report and suggested guidelines from the International workshop on the safety of repetitive transcranial magnetic stimulation, June 5-7, 1996. Electroencephalogr Clin Neurophysiol. 1998;108(1):1–16. https://doi.org/10.1016/s0168-5597(97)00096-8
34 Rossi S, Antal A, Bestmann S, Bikson M, Brewer C, Brockmöller J, et al. Safety and recommendations for TMS use in healthy subjects and patient populations, with updates on training, ethical and regulatory issues: expert guidelines. Clin Neurophysiol. 2021;132(1):269–306. https://doi.org/10.1016/j.clinph.2020.10.003
35 Rossi S, Hallett M, Rossini PM, Pascual-Leone A. Safety, ethical considerations, and application guidelines for the use of transcranial magnetic stimulation in clinical practice and research. Clin Neurophysiol. 2009;120(12):2008–39. https://doi.org/10.1016/j.clinph.2009.08.016
36 Van Hoornweder S, Geraerts M, Verstraelen S, Nuyts M, Caulfield KA, Meesen R. From scalp to cortex, the whole isn't greater than the sum of its parts: introducing get tissue thickness (GTT) to assess age and sex differences in tissue thicknesses. bioRxiv. 2023. https://doi.org/10.1101/2023.04.18.537177
37 Esty W. Elements of electricity: a practical discussion of the fundamental laws and phenomena of electricity and their practical applications in the business and industrial world. American Technical Society; 1944.
38 Aldridge BG, Waldman GS, Physics AIO. Automobile ignition System: a module on electricity and magnetism. McGraw-Hill; 1975.
39 Bijsterbosch JD, Barker AT, Lee KH, Woodruff PWR. Where does transcranial magnetic stimulation (TMS) stimulate? Modelling of induced field maps for some common cortical and cerebellar targets. Med Biol Eng Comput. 2012;50(7):671–81. https://doi.org/10.1007/s11517-012-0922-8
40 Roth BJ, Cohen LG, Hallett M. The electric field induced during magnetic stimulation. Electroencephalogr Clin Neurophysiol Suppl. 1991;43:268–78.
41 George MS, Wassermann EM, Kimbrell TA, Little JT, Williams WE, Danielson AL, et al. Mood improvement following daily left prefrontal repetitive transcranial magnetic stimulation in patients with depression: a placebo-controlled crossover trial. Am J Psychiatry. 1997;154(12):1752–6. https://doi.org/10.1176/ajp.154.12.1752
42 Padberg F, Zwanzger P, Thoma H, Kathmann N, Haag C, D. Greenberg B, et al. Repetitive transcranial magnetic stimulation (rTMS) in pharmacotherapy-refractory major depression: comparative study of fast, slow and sham rTMS. Psychiatry Res. 1999; 88(3):163–71. https://doi.org/10.1016/s0165-1781(99)00092-x
43 Eschweiler GW, Wegerer C, Schlotter W, Spandl C, Stevens A, Bartels M, et al. Left prefrontal activation predicts therapeutic effects of repetitive transcranial magnetic stimulation (rTMS) in major depression. Psychiatry Res. 2000;99(3):161–72. https://doi.org/10.1016/s0925-4927(00)00062-7

Downloaded from http://karger.com/pps/article-pdf/doi/10.1159/000552942/4545790/000552942.pdf by Max Planck Society user on 27 July 2026

44 Berman RM, Narasimhan M, Sanacora G, Miano AP, Hoffman RE, Hu X, et al. A randomized clinical trial of repetitive transcranial magnetic stimulation in the treatment of major depression. Biol Psychiatry. 2000;47(4):332–7. https://doi.org/10.1016/s0006-3223(99)00243-7
45 Padberg F. Repetitive transcranial magnetic stimulation (rTMS) in major depression: relation between efficacy and stimulation intensity. Neuropsychopharmacology. 2002;27(4):638–45. https://doi.org/10.1016/s0893-133x(02)00338-x
46 Boutros NN, Gueorguieva R, Hoffman RE, Oren DA, Feingold A, Berman RM. Lack of a therapeutic effect of a 2-week sub-threshold transcranial magnetic stimulation course for treatment-resistant depression. Psychiatry Res. 2002;113(3):245–54. https://doi.org/10.1016/s0165-1781(02)00267-6
47 Höppner J, Schulz M, Irmisch G, Mau R, Schläfke D, Richter J. Antidepressant efficacy of two different rTMS procedures. High frequency over left versus low frequency over right prefrontal cortex compared with sham stimulation. Eur Arch Psychiatry Clin Neurosci. 2003;253(2):103–9. https://doi.org/10.1007/s00406-003-0416-7
48 Fitzgerald PB, Brown TL, Marston NAU, Daskalakis ZJ, de Castella A, Kulkarni J. Transcranial magnetic stimulation in the treatment of depression: a double-blind, placebo-controlled trial. Arch Gen Psychiatry. 2003;60(10):1002–8. https://doi.org/10.1001/archpsyc.60.9.1002
49 Holtzheimer PE 3rd, Russo J, Claypoole KH, Roy-Byrne P, Avery DH. Shorter duration of depressive episode may predict response to repetitive transcranial magnetic stimulation. Depress Anxiety. 2004;19(1):24–30. https://doi.org/10.1002/da.10147
50 Rossini D, Lucca A, Zanardi R, Magri L, Smeraldi E. Transcranial magnetic stimulation in treatment-resistant depressed patients: a double-blind, placebo-controlled trial. Psychiatry Res. 2005;137(1–2):1–10. https://doi.org/10.1016/j.psychres.2005.06.008
51 Möller AL, Hjaltason Ó, Ívarsson Ó, Stefánsson SB. The effects of repetitive transcranial magnetic stimulation on depressive symptoms and the P(300) event-related potential. Nord J Psychiatry. 2006;60(4):282–5. https://doi.org/10.1080/08039480600790119
52 Avery DH, Holtzheimer PE III, Fawaz W, Russo J, Neumaier J, Dunner DL, et al. A controlled study of repetitive transcranial magnetic stimulation in medication-resistant major depression. Biol Psychiatry. 2006;59(2):187–94. https://doi.org/10.1016/j.biopsych.2005.07.003
53 Loo CK, Mitchell PB, Mcfarquhar TF, Malhi GS, Sachdev PS. A sham-controlled trial of the efficacy and safety of twice-daily rTMS in major depression. Psychol Med. 2007;37(3):341–9. https://doi.org/10.1017/s0033291706009597
54 Bortolomasi M, Minelli A, Fuggetta G, Perini M, Comencini S, Fiaschi A, et al. Long-lasting effects of high frequency repetitive transcranial magnetic stimulation in major depressed patients. Psychiatry Res. 2007;150(2):181–6. https://doi.org/10.1016/j.psychres.2006.04.010
55 Stern WM, Tormos JM, Press DZ, Pearlman C, Pascual-Leone A. Antidepressant effects of high and low frequency repetitive transcranial magnetic stimulation to the dorsolateral prefrontal cortex: a double-blind, randomized, placebo-controlled trial. J Neuropsychiatry. 2007;19(2):179–86. https://doi.org/10.1176/appi.neuropsych.19.2.179
56 Mogg A, Pluck G, Eranti S, Landau S, Purvis R, Brown R, et al. A randomized controlled trial with 4-month follow-up of adjunctive repetitive transcranial magnetic stimulation of the left prefrontal cortex for depression. Psychol Med. 2008;38(3):323–33. https://doi.org/10.1017/s0033291707001663
57 Narushima K, McCormick LM, Yamada T, Thatcher RW, Robinson RG. Subgenual cingulate theta activity predicts treatment response of repetitive transcranial magnetic stimulation in participants with vascular depression. J Neuropsychiatry Clin Neurosci. 2010;22(1):75–84. https://doi.org/10.1176/jnp.2010.22.1.75
58 Pal E, Nagy F, Aschermann Z, Balazs E, Kovacs N. The impact of left prefrontal repetitive transcranial magnetic stimulation on depression in Parkinson's disease: a randomized, double-blind, placebo-controlled study. Mov Disord. 2010;25(14):2311–7. https://doi.org/10.1002/mds.23270
59 Zheng H, Zhang L, Li L, Liu P, Gao J, Liu X, et al. High-frequency rTMS treatment increases left prefrontal myo-inositol in young patients with treatment-resistant depression. Prog Neuropsychopharmacol Biol Psychiatry. 2010;34(7):1189–95. https://doi.org/10.1016/j.pnpbp.2010.06.009
60 Hoeppner J, Padberg F, Domes G, Zinke A, Herpertz SC, Großheinrich N, et al. Influence of repetitive transcranial magnetic stimulation on psychomotor symptoms in major depression. Eur Arch Psychiatry Clin Neurosci. 2010;260(3):197–202. https://doi.org/10.1007/s00406-009-0039-8
61 Leyman L, De Raedt R, Vanderhasselt MA, Baeken C. Effects of repetitive transcranial magnetic stimulation of the dorsolateral prefrontal cortex on the attentional processing of emotional information in major depression: a pilot study. Psychiatry Res. 2011;185(1–2):102–7. https://doi.org/10.1016/j.psychres.2009.04.008
62 Peng H, Zheng H, Li L, Liu J, Zhang Y, Shan B, et al. High-frequency rTMS treatment increases white matter FA in the left middle frontal gyrus in young patients with treatment-resistant depression. J Affect Disord. 2012;136(3):249–57. https://doi.org/10.1016/j.jad.2011.12.006
63 Kreuzer PM, Langguth B, Schecklmann M, Eichhammer P, Hajak G, Landgrebe M. Can repetitive transcranial magnetic stimulation prolong the antidepressant effects of sleep deprivation? Brain Stimul. 2012;5(2):141–7. https://doi.org/10.1016/j.brs.2011.02.005
64 Baeken C, Vanderhasselt MA, Remue J, Herremans S, Vanderbruggen N, Zeeuws D, et al. Intensive HF-rTMS treatment in refractory medication-resistant unipolar depressed patients. J Affect Disord. 2013;151(2):625–31. https://doi.org/10.1016/j.jad.2013.07.008
65 Chen ST, Shaw-Ji C, Chun-Hung C, Hsin-Chi T, Lin CCH. Superior antidepressant effect occurring 1 month after rTMS: add-on rTMS for subjects with medication-resistant depression. Neuropsychiatr Dis Treat. 2013;9:397–401. https://doi.org/10.2147/ndt.s40466
66 Speer AM, Wassermann EM, Benson BE, Herscovitch P, Post RM. Antidepressant efficacy of high and low frequency rTMS at 110% of motor threshold versus sham stimulation over left prefrontal cortex. Brain Stimul. 2014;7(1):36–41. https://doi.org/10.1016/j.brs.2013.07.004
67 Desmyter S, Duprat R, Baeken C, Bijttebier S, van Heeringen K. The acute effects of accelerated repetitive transcranial magnetic stimulation on suicide risk in unipolar depression: preliminary results. Psychiatr Danub. 2014;26(Suppl 1):48–52.
68 Levkovitz Y, Isserles M, Padberg F, Lisanby SH, Bystritsky A, Xia G, et al. Efficacy and safety of deep transcranial magnetic stimulation for major depression: a prospective multicenter randomized controlled trial. World Psychiatry. 2015;14(1):64–73. https://doi.org/10.1002/wps.20199
69 Blumberger DM, Maller JJ, Thomson L, Mulsant BH, Rajji TK, Maher M, et al. Unilateral and bilateral MRI-targeted repetitive transcranial magnetic stimulation for treatment-resistant depression: a randomized controlled study. J Psychiatry Neurosci. 2016;41(4):E58–66. https://doi.org/10.1503/jpn.150265
70 Duprat R, Desmyter S, Rudi DR, van Heeringen K, Van den Abbeele D, Tandt H, et al. Accelerated intermittent theta burst stimulation treatment in medication-resistant major depression: a fast road to remission? J Affect Disord. 2016;200:6–14. https://doi.org/10.1016/j.jad.2016.04.015
71 Taylor SF, Ho SS, Abagis T, Angstadt M, Maixner DF, Welsh RC, et al. Changes in brain connectivity during a sham-controlled, transcranial magnetic stimulation trial for depression. J Affect Disord. 2018;232:143–51. https://doi.org/10.1016/j.jad.2018.02.019

Downloaded from http://karger.com/pps/article-pdf/doi/10.1159/000552942/4545790/000552942.pdf by Max Planck Society user on 27 July 2026

72 Pan F, Shen Z, Jiao J, Chen J, Li S, Lu J, et al. Neuronavigation-guided rTMS for the treatment of depressive patients with suicidal ideation: a double-blind, randomized, sham-controlled trial. Clin Pharmacol Ther. 2020; 108(4):826–32. https://doi.org/10.1002/cpt.1858
73 van Eijndhoven PFP, Bartholomeus J, Möbius M, de Bruijn A, Ferrari G, Mulders P, et al. A randomized controlled trial of a standard 4-week protocol of repetitive transcranial magnetic stimulation in severe treatment resistant depression. J Affect Disord. 2020;274:444–9. https://doi.org/10.1016/j.jad.2020.05.055
74 Li CT, Cheng CM, Juan CH, Tsai YC, Chen MH, Bai YM, et al. Task-modulated brain activity predicts antidepressant responses of prefrontal repetitive transcranial magnetic stimulation: a randomized sham-control study. Chronic Stress. 2021;5:24705470211006855. https://doi.org/10.1177/24705470211006855
75 Dalhuisen I, Ackermans E, Martens L, Mulders P, Bartholomeus J, de Bruijn A, et al. Longitudinal effects of rTMS on neuroplasticity in chronic treatment-resistant depression. Eur Arch Psychiatry Clin Neurosci. 2021;271(1):39–47. https://doi.org/10.1007/s00406-020-01135-w
76 Tong J, Zhang J, Jin Y, Liu W, Wang H, Huang Y, et al. Impact of repetitive transcranial magnetic stimulation (rTMS) on theory of mind and executive function in major depressive disorder and its correlation with brain-derived neurotrophic factor (BDNF): a randomized, double-blind, Sham-controlled trial. Brain Sci. 2021;11(6):765. https://doi.org/10.3390/brainsci11060765
77 Chen Y, Li X, Wang L, Tian S, Chen Y, Wang F, et al. Effects of repetitive transcranial magnetic stimulation on cognitive function in patients with stress-related depression: a randomized double-blind fMRI and 1H-MRS study. Front Neurol. 2022;13:844606. https://doi.org/10.3389/fneur.2022.844606
78 Yu F, Huang Y, Chen T, Wang X, Guo Y, Fang Y, et al. Repetitive transcranial magnetic stimulation promotes response inhibition in patients with major depression during the stop-signal task. J Psychiatr Res. 2022;151:427–38. https://doi.org/10.1016/j.jpsychires.2022.05.014
79 Yesavage JA, Fairchild JK, Mi Z, Biswas K, Davis-Karim A, Phibbs CS, et al. Effect of repetitive transcranial magnetic stimulation on treatment-resistant major depression in US veterans: a randomized clinical trial. JAMA Psychiatry. 2018;75(9):884–93. https://doi.org/10.1001/jamapsychiatry.2018.1483
80 Dai L, Wang P, Zhang P, Guo Q, Du H, Li F, et al. The therapeutic effect of repetitive transcranial magnetic stimulation in elderly depression patients. Medicine. 2020;99(32): e21493. https://doi.org/10.1097/md.0000000000021493
81 Zhao Y, He Z, Luo W, Yu Y, Chen J, Cai X, et al. Effect of intermittent theta burst stimulation on suicidal ideation and depressive symptoms in adolescent depression with suicide attempt: a randomized sham-controlled study. J Affect Disord. 2023;325: 618–26. https://doi.org/10.1016/j.jad.2023.01.061
82 Li X, Liu J, Wei S, Yu C, Wang D, Li Y, et al. Cognitive enhancing effect of rTMS combined with tDCS in patients with major depressive disorder: a double-blind, randomized, sham-controlled study. BMC Med. 2024;22(1):253. https://doi.org/10.1186/s12916-024-03443-7
83 Li K, Mo D, Yu Q, Feng R, Li Y. Effect of repetitive transcranial magnetic stimulation on post-stroke comorbid cognitive impairment and depression: a randomized controlled trial. J Alzheimers Dis. 2024;101(1): 337–52. https://doi.org/10.3233/jad-240505
84 Liu X, Peng Z, Cheng F, Li G, Wang B, Hu C, et al. Efficacy and safety of accelerated intermittent theta-burst stimulation for adolescents with major depressive disorder: a randomized, double-blind, Sham-controlled study. Biol Psychiatry. 2026; 99(3):218–26. https://doi.org/10.1016/j.biopsych.2025.07.018
85 Zhang M, Li W, Ye Y, Hu Z, Zhou Y, Ning Y. Efficacy and safety of intermittent theta burst stimulation on adolescents and young adults with major depressive disorder: a randomized, double blinded, controlled trial. J Affect Disord. 2024;350:214–21. https://doi.org/10.1016/j.jad.2024.01.025
86 Huang X, Xi C, Fang Y, Ye R, Wang X, Zhang S, et al. Therapeutic efficacy of reward circuit-targeted transcranial magnetic stimulation (TMS) on suicidal ideation in depressed patients: a Sham-controlled trial of two TMS protocols. Depress Anxiety. 2025; 2025(1):1767477. https://doi.org/10.1155/da/1767477
87 Liu X, Li P, Xia Y, Yuan S, Chen C, Xie K, et al. Efficacy study of intermittent theta burst stimulation (iTBS) in the treatment of adolescents with affective disorders. J Affect Disord. 2025;373:284–90. https://doi.org/10.1016/j.jad.2025.01.002
88 Maciaszek J, Rymaszewska J, Wieczorek T, Piotrowski P, Szcześniak D, Beszłej JA, et al. Preliminary findings of a randomized controlled trial investigating the efficacy of transcranial magnetic stimulation in treatment-resistant depression: a post-hoc analysis on the role of co-occurring personality disorders. Front Psychiatr. 2024;15: 1363984. https://doi.org/10.3389/fpsyt.2024.1363984
89 Tura A, Promet L, Goya-Maldonado R. Structural-functional connectomics in major depressive disorder following aiTBS treatment. Psychiatry Res. 2024;342:116217. https://doi.org/10.1016/j.psychres.2024.116217
90 Gomez LJ, Dannhauer M, Koponen LM, Peterchev AV. Conditions for numerically accurate TMS electric field simulation. Brain Stimul. 2020;13(1):157–66. https://doi.org/10.1016/j.brs.2019.09.015
91 Stokes MG, Chambers CD, Gould IC, English T, McNaught E, McDonald O, et al. Distance-adjusted motor threshold for transcranial magnetic stimulation. Clin Neurophysiol. 2007;118(7):1617–25. https://doi.org/10.1016/j.clinph.2007.04.004
92 Numssen O, Kuhnke P, Weise K, Hartwigsen G. Electric-field-based dosing for TMS. Imaging Neurosci. 2024;2:106. https://doi.org/10.1162/imag_a_00106
93 Janssen AM, Rampersad SM, Lucka F, Lanfer B, Lew S, Aydin Ü, et al. The influence of sulcus width on simulated electric fields induced by transcranial magnetic stimulation. Phys Med Biol. 2013;58(14):4881–96. https://doi.org/10.1088/0031-9155/58/14/4881
94 Rashed EA, Gomez-Tames J, Hirata A. Influence of segmentation accuracy in structural MR head scans on electric field computation for TMS and tES. Phys Med Biol. 2021;66(6):064002. https://doi.org/10.1088/1361-6560/abe223
95 Dannhauer M, Gomez LJ, Robins PL, Wang D, Hasan NI, Thielscher A, et al. Electric field modeling in personalizing transcranial magnetic stimulation interventions. Biol Psychiatry. 2024;95(6):494–501. https://doi.org/10.1016/j.biopsych.2023.11.022
96 McCalley DM, Cadicamo NJ, Weijerman F, Tenekedjieva LT, Knutson B, Padula CB. Females have shorter scalp-to-cortex distances and receive stronger TMS electrical fields: implications for clinical treatment. Neuropsychopharmacology. 2026;51(4): 722–31. https://doi.org/10.1038/s41386-025-02299-6
97 Hermsen AM, Haag A, Duddek C, Balkenhol K, Bugiel H, Bauer S, et al. Test-retest reliability of single and paired pulse transcranial magnetic stimulation parameters in healthy subjects. J Neurol Sci. 2016; 362:209–16. https://doi.org/10.1016/j.jns.2016.01.039
98 Grosshagauer S, Woletz M, Vasileiadi M, Linhardt D, Nohava L, Schuler AL, et al. Chronometric TMS-fMRI of personalized left dorsolateral prefrontal target reveals state-dependency of subgenual anterior cingulate cortex effects. Mol Psychiatry. 2024;29(9):2678–88. https://doi.org/10.1038/s41380-024-02535-3
99 Schuler A-L, Tik M, Kallioniemi E, Suller Marti A, Cai Z, Pellegrino G. Approaches to map cortical excitability beyond the primary motor cortex – perspectives from cognitive neuroscience, multimodal imaging and clinical applications. Neurosci Biobehav Rev. 2025;177:106338. https://doi.org/10.1016/j.neubiorev.2025.106338

Downloaded from http://karger.com/pps/article-pdf/doi/10.1159/000552942/4545790/000552942.pdf by Max Planck Society user on 27 July 2026